This paper was presented at:

The Ninth International Symposium on Magnetic Bearings (ISMB9)
Hosted by the University of Kentucky
Radisson Plaza Hotel Lexington KY, USA
August 3-6, 2004

SPIN COMMISSIONING AND DROP TESTS OF A 130 kW-hr COMPOSITE FLYWHEEL

Matthew T. Caprio, Brian T. Murphy, John D. Herbst
The University of Texas at Austin, Center for Electromechanics
1 University Station R7000, Austin, TX 78712
mcaprio@mail.utexas.edu

ABSTRACT

The Center for Electromechanics at the University of Texas at Austin is developing a power averaging flywheel battery for use on high speed passenger trains as part of the Federal Railroad Administration's Next Generation High Speed Rail Program. The flywheel rotor, which weighs 5100 lb, is designed to store 130 kW-hr of energy at a peak design speed of 15,000 rpm. The graphite-epoxy composite rotor, which runs in a vacuum, is supported by a 5 axis active magnetic bearing system. A high speed 2 MW motor-generator, which is outside the vacuum, is directly coupled to the flywheel with an industrial disk pack coupling, through a custom integral rotary vacuum seal.

This paper begins with a brief description of the design of the vertically oriented flywheel rotor/housing system. The partially complete rotor (currently 3000 lb mass) has recently been undergoing system level laboratory commissioning. Test results are presented demonstrating the performance of the magnetic bearings. Since flywheel system safety is such a critical issue at this energy level, satisfactory performance of the backup bearings was demonstrated experimentally. Delevitation "drop" tests have been performed onto rolling element backup bearings, and behavior is reported and compared to related flywheels discussed in the literature. Finally, testing of a semi-passive whirl arresting scheme is presented.

FLYWHEEL SYSTEM DESCRIPTION

The ALPS flywheel is the energy storage component of a hybrid-electric locomotive power system for use in a high speed passenger rail application [1]. The design speed range of the flywheel is 7500-15000 rpm, providing 100 kW-hr of delivered energy at up to 2 MW power rating [2]. To withstand the spin stresses of the supersonic tip speed, the main rotor body is constructed of filament wound graphite-epoxy composite [3].

The vertically oriented rotor is supported by a 5 axis active magnetic bearing system employing permanent magnet bias homopolar radial bearings and a double-acting PM bias thrust bearing [4]. To support the rotor while at rest or in the event of a magnetic bearing system fault, a set of rolling element backup bearings is mounted at each shaft end. The backup bearings are mounted in oil squeeze film dampers to reduce impact loading on the bearings during a delevitation, and increase bearing life. A cutaway section of the ALPS flywheel with the full 15 ring rotor can be seen in Figure 1, showing the main components of the magnetic bearing and backup bearing systems. The internal composite burst liner and external motor generator are not shown.

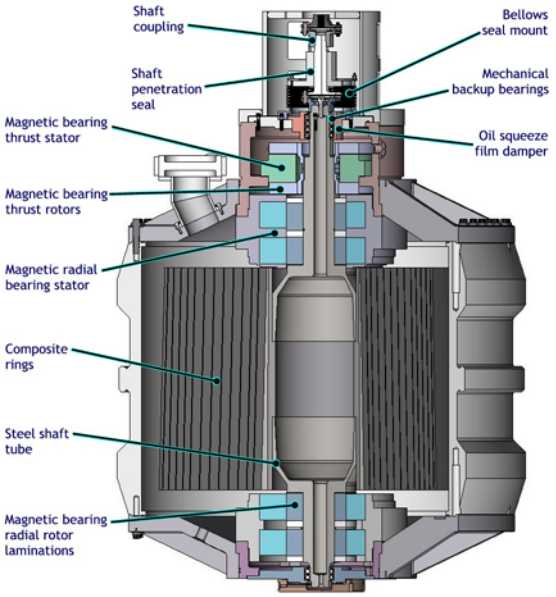

Figure 1. ALPS flywheel rotor and magnetic bearing system

LABORATORY TESTING

In the interest of safety, the test plan of the ALPS flywheel calls for two phases of commissioning and laboratory spin testing before eventual integration of the flywheel into the locomotive for "rolling demonstrations" in the dynamic environment. "Intermediate spin testing", the first laboratory testing phase, is designed to exercise all flywheel systems and

components at full speed, though at reduced energy levels, through the use of the partially constructed 3000 lb rotor. This paper discusses only this current phase of testing.

The partial rotor for intermediate spin testing consists of only the first 6 of the final 15 composite rings installed on the rotor shaft assembly, providing a maximum energy of approximately 25 kW-hr at full design speed. The burst liner is not installed into the flywheel housing for this phase of testing as the full energy of the rotor in this configuration can be safely contained by the stainless steel vessel in the unlikely event of a ring burst. These tests are performed in the CEM concrete spin test facility, with the housing mounted rigidly to the mount structure by way of pedestal struts. Figure 2 shows the ALPS flywheel in the CEM spin test bunker during intermediate spin testing. In place of the motor generator, a 400 HP hydraulic motoring system and speed increasing gearbox provide the drive for this phase of low power, low energy, full speed testing.

The goals of intermediate spin testing are to: 1) demonstrate the rotordynamic performance of the flywheel, 2) commission and tune the magnetic bearing system, 3) test the effectiveness of the backup bearing system, 4) collect experimental data on the thermal management of rotor losses to determine maximum allowable run time, and 5) evaluate the performance of auxiliary systems.

To date, the flywheel has been successfully commissioned to a speed of 13,600 rpm. Only minor tuning of the magnetic bearing compensator has been necessary as the measured transfer functions have closely matched the predicted modes. Auxiliary systems, including the vacuum system, shaft seal, seal compliant bellows mount, and the radial bearing stator water-cooling system have functioned well.

While the stability and controllability of the rotor has been satisfactory, a mode of the coupling set required attention. With the hydraulic motor and speed-increasing gearbox installed in place of the motor generator, a flexible coupling mode exists within the operating speed range. This 180 Hz (10800 cpm) mode is dominated by the flexibility of the gearbox output shaft and resulted in large response of the coupling set. A custom designed plate-type viscous damper was mounted to the seal housing to attenuate the response and allow safe passage through the resonance at 10800 rpm shaft speed.

Currently, endurance tests are underway to measure the operating temperatures of the magnetic bearing stator and rotor components during extended periods of operation at numerous fixed speeds. As the rotor laminations rely on passive radiation cooling, the maximum run time of the flywheel is expected to be limited by the peak allowable temperatures of this component. Since the magnetic materials employed in these high speed bearing laminations are not well characterized, there is a significant amount of uncertainty in the bearing hysteresis and eddy current loss predictions. Thus, experimental data from the endurance runs will be incorporated into the thermal model of the rotor to refine the predictions of the magnetic bearing losses.

Figure 2. ALPS flywheel in laboratory spin testing

DROP TESTING

The backup bearing system of the ALPS flywheel is essential for the safe shutdown of the flywheel in the event of a magnetic bearing system failure. The system is necessary to provide the critical function of supporting the rotor for the approximately 5 minutes required to discharge the flywheel from full energy in the event of loss of magnetic bearing control.

For this reason, great care was taken in the selection of the rolling element backup bearings and the design of their squeeze film damper supporting components to provide adequate load capacity and design life. Further, as catastrophic unstable backward whirl behavior on the backup bearings has been recognized in other flywheels [5,6], modeling and simulations were carried out to predict the performance of the backup bearings during the design stage. However, simulation of the backup bearing performance yielded ineffective results as the predicted behavior was shown to be very strongly dependent on terms with large uncertainty, such as the dynamic coefficient of friction at the shaft-inner race interface.

Behavior of the rotor on the backup bearings was thus demonstrated experimentally. Delevitation tests were performed at speeds between 10 and 5000 rpm, dropping the rotor onto the backup bearings and allowing whirl motion to reach steady state. Unexpectedly, in all cases the rotor whirled *forward* (in the direction of rotation) around the 0.020" radial (0.5 mm) backup bearing clearance circle. Reverse whirl was never seen while operating on the backup bearings. Typical orbit diameter is less than 2 mils during normal operation. Figure 3 shows an X-Y orbit plot of a delevitation and relevitation at 2000 rpm (note direction of shaft rotation is clockwise).

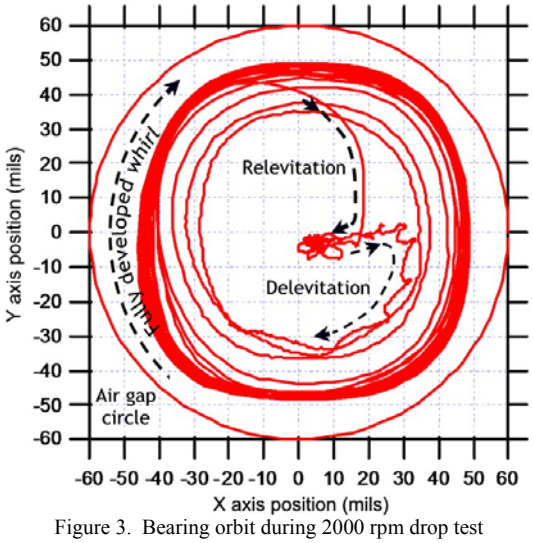

Figure 3. Bearing orbit during 2000 rpm drop test

For these tests, delevitation was achieved by ramping the controller gains to zero. Upon this action, the rotor contacts the backup bearings in about 250 ms. Forward whirl begins immediately and takes about 5-6 orbits to fully develop. At shaft speeds up to 1500 rpm, the forward whirl rate was slightly sub-synchronous (98-99%). For speeds from 1500 to 5000 rpm, the steady state forward whirl rate reached a plateau of 28.3 Hz (1698 cpm). Multiple drop tests were performed at each shaft speed, and both the whirl rate and orbit size exhibited were consistent and repeatable. Figure 4 summarizes the whirl rate and orbit size obtained at the numerous speeds of the drop tests.

The size of the orbit of the rotor was measured at the radial bearing locations by the collocated optical position feedback sensors. Due to flexibility of the shaft and deflection of the squeeze film dampers, the rotor orbit during whirling is significantly larger than simply the backup bearing clearance, but less than the actuator air gap.

A significant conclusion drawn from the drop tests is that the forward whirl rate of the rotor operating on the backup bearings is naturally limited to less than 30 Hz, apparently independent of shaft speed. This is noteworthy in that it implies that the orbit size while whirling is bounded, in this case to a value less than the radial bearing air gap of 0.060" (1.52 mm). Were the whirl rate to continue increasing for drops at higher speeds, the correspondingly larger orbit (eccentricity) would result in higher centrifugal loads and shaft deflection, eventually causing contact between the bearing laminations and stator.

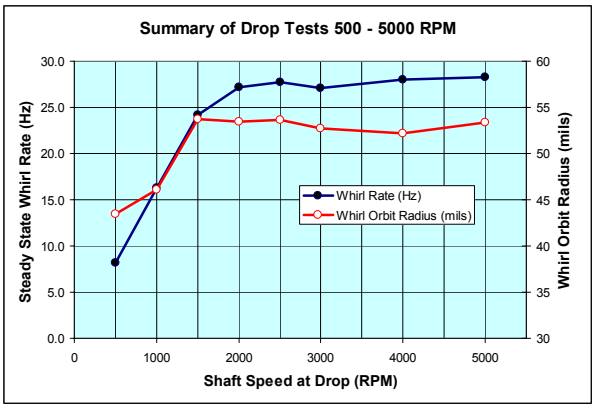

Figure 4. Whirl rates and orbits exhibited through drop tests

In an attempt to explain the cause of forward whirl, and the natural plateau of the whirl rate, an extensive literature search of backup bearing drop tests was conducted. First note that backup bearing contact is excluded as a cause for forward whirl by Maslen's comment that whirl induced by contact friction can only be reverse whirl [7] as friction acts in the direction opposite to rotation. According to Schmied, [8] the cause of forward whirl while operating on backup bearings is running with a large imbalance. Swanson [9] took this point further by correlating the amount of imbalance with the resulting whirl direction and rates for horizontal rotors. In these drop tests, large imbalances were necessary to cause forward whirl on ball bearings or solid bushings; the balanced rotors (or only slightly imbalanced) did not whirl at all. Further, Kirk [10] notes that during a drop, the outward spiraling action of a rotor accelerating toward the backup bearings through the clearance distance provides added momentum to forward whirl. From these studies, it is apparent that forward whirl on backup bearings *can* be excited by imbalance, or the spiraling that occurs during the delevitation before the backup bearings are engaged.

While imbalance may indeed be a general cause of forward whirl, the ALPS rotor was dynamically balanced in two planes before operation, trimming the inertial center to within 0.1 mils of the rotational center, suggesting that another mechanism may drive forward whirl in this application.

Only Kirk and Swanson's work [9] was found to identify specific forward whirl rates. While these

results repeatably demonstrated sub-synchronous forward whirl for a number of different drop cases, they are all presented for the same operating speed (4000 rpm). It is therefore unclear if the sub-synchronous whirl rates were limited or independent of speed.

There is however, a very clear consensus in the literature regarding the determining factor of *reverse* whirl frequency. Foiles [11], Fumagalli [12], Maslen [7], Ishii [13], and Bartha [14] all mention that for a compliantly supported bearing stator, the theoretical and experimental results show that reverse whirl quickly "locks in" to the first elastic eigenfrequency of the combined rotor/stator system (with bearing clearance dead band omitted). Although reverse whirl is theoretically bounded only by the kinematic rolling condition (an extremely high frequency), in application the natural frequency of the rotor/stator system strongly determines and limits the reverse whirl rate. Bartha [14] presents a theoretical method to predict maximum (reverse) whirl rate vs. rotational frequency and compares it to experimental results, yielding excellent agreement. These results demonstrate that the maximum whirl rate is bounded and occurs at an intermediate rotor speed and drops slightly with increased speed. Applying this behavior to the case of forward whirl, we can postulate that once forward whirl momentum is established, a combined rotor/housing system mode will also control the forward whirl rate.

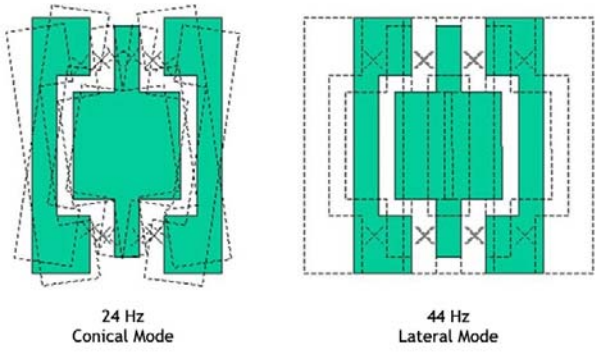

Figure 5. Rigid body housing modes identified by rap tests

This working theory suggests that a system mode may be responsible for limiting the maximum forward whirl rate of the ALPS flywheel to approximately 28 Hz. With the rotor supported on the backup bearings, rap tests of the flywheel housing in the spin test mount pedestals identified two rigid body housing modes with shapes as shown in Figure 5. The close vicinity of the 24 Hz housing mode to the 28 Hz whirl rate plateau suggests that this mode is likely dictating the whirl rate of the rotor on the backup bearings. Plausible explanations for modification of this mode from 24 to 28 Hz may exist in nonlinearity of the system at large deflections (as those experienced during large orbit whirling), or in the variation of the phase relationship between the rotor and housing at various shaft speeds.

During the course of drop testing, no cases of 44 Hz whirl were exhibited. Indeed, no whirl rates were seen above 28 Hz whatsoever, despite the fact that several tests were conducted at rotor speeds above 44 Hz. Specifically, the 3000 rpm (50 Hz), 4000 (66.7 Hz), and 5000 (83.3 Hz) drop tests all locked into the 27-28 Hz whirl rate. This point is significant in that it appears to indicate that the 24 Hz conical mode dominates over the 44 Hz lateral mode (and other, less pronounced, higher frequency modes) with regard to dictating whirl rate. This suggests that the whirl rate is likely limited to 28 Hz for drops at all speeds *above* 5000 rpm as well.

Confirmation of the theory of the conical housing mode determining the maximum whirl rate may be obtained during future testing of the flywheel while mounted in a two axis gimbal mount. The gimbal mount and the associated shock isolation system are required to minimize gyroscopic and shock loads due to locomotive chassis motions during dynamic testing. When the mount properties are altered, the housing natural frequency will be modified, and a corresponding change in the maximum whirl rate is expected. In order to isolate the flywheel from the locomotive vibration environment, the shock isolation system is targeted with a natural frequency of 15 Hz, implying that for the final installation, the maximum whirl rate may be in the neighborhood of 15 Hz.

SEMI-PASSIVE WHIRL ARREST

In addition to empirical and analytical characterization of rotor dynamic behavior on the touchdown bearings, a semi-passive whirl arresting scheme was devised and tested to allow the operators to manually stop whirling motion during a magnetic bearing fault. This system is useful because sustained whirling operation for prolonged periods is undesirable, regardless of whirl rates and orbit size.

Higher loading on the shaft and backup bearings (reducing bearing life) is one reason to avoid sustained whirling. Also, the whirling action of the rotor in the permanent magnet bias field of the actuator can generate undesirable back EMF, predictable by the equation for the voltage across the coil of a bearing actuator [15]. This unanticipated phenomenon occurred during some drop tests while whirling at approximately 27 Hz. Back-EMF in the system freewheeled through the power amplifiers and overcharged the power supply capacitors, causing built-in protection features of the power amplifiers to "trip-out". Relevitation could not take place until the over voltage was dissipated. Thus, to enhance system reliability by improving the chances of being able to relevitate after a drop, additional

devices were added to the magnetic bearing power electronics to shunt regenerative currents.

A further reason to arrest whirl in the ALPS flywheel system is that the dynamic load capacity of the radial bearings is marginal for re-centering the rotor from large orbits at about 30 Hz (while the forward whirl rate is limited to approximately 28 Hz). Therefore, the ability to re-center the rotor after clearing a magnetic bearing fault is much improved if the rotor is captured rather than whirling.

Many works [10,11,12,16] demonstrate the theoretical and experimental effectiveness of the gravity field in preventing whirl (both forward and reverse) in horizontal rotor systems. The cause for this [12] is that the energy converted to reverse whirl through friction (minus the whirl energy dissipated in the backup bearing dampers) can be insufficient to overcome the potential energy required to lift the rotor out of the bottom half of the backup bearing orbits.

Although the ALPS rotor is vertical, this same principle of a "gravity" field was synthetically applied to arrest whirl. By generating a preferred radial orientation of the rotor through a DC bias field created by the control coils, a similar effect is imposed on the rotor. With this approach, the rotor is pulled preferentially into a particular radial quadrant, and a potential energy well is produced which arrests the whirling rotor.

A manually switched passive whirl arresting circuit was created and installed in the magnetic bearing cabinet. The action replaces the command inputs from the active magnetic bearing (AMB) compensator to the power amplifiers with fixed (but adjustable) constant current commands, as shown in Figure 6.

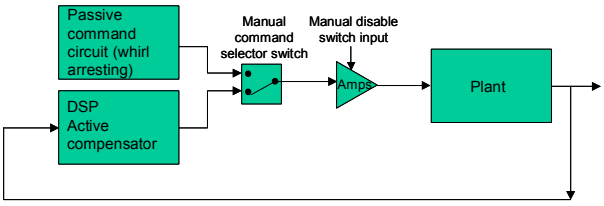

Figure 6. Whirl arrest schematic

The passive current command result in a force pushing the rotor into the +X,+Y quadrant of both radial bearings. By influencing the rotor to stay in one quadrant, this circuit has been shown to arrest the whirling rotor within a few whirl cycles, at all drop test speeds. The semi-passive whirl arrest circuit may provide protection against whirling in the case of a fault of the bearing controller, loss of a position sensor, or possibly loss of amplifiers (if a sufficiently high DC current level is used on the remaining amplifiers).

Testing of the whirl arrest system began at 500 rpm where it was found that a minimum of 1.2 amps of current was required to arrest fully developed whirl. The current required to stop whirl was found to increase as speed increased, eventually requiring 5 amps at 2000 rpm (25% of maximum dynamic radial bearing current for this system). Further testing at speeds up to 5000 rpm, demonstrated that 5 amps was sufficient to arrest fully developed whirl. It is believed that the required current does not continue to increase as speed increases because the whirl rate was found to remain essentially capped at close to 28 Hz.

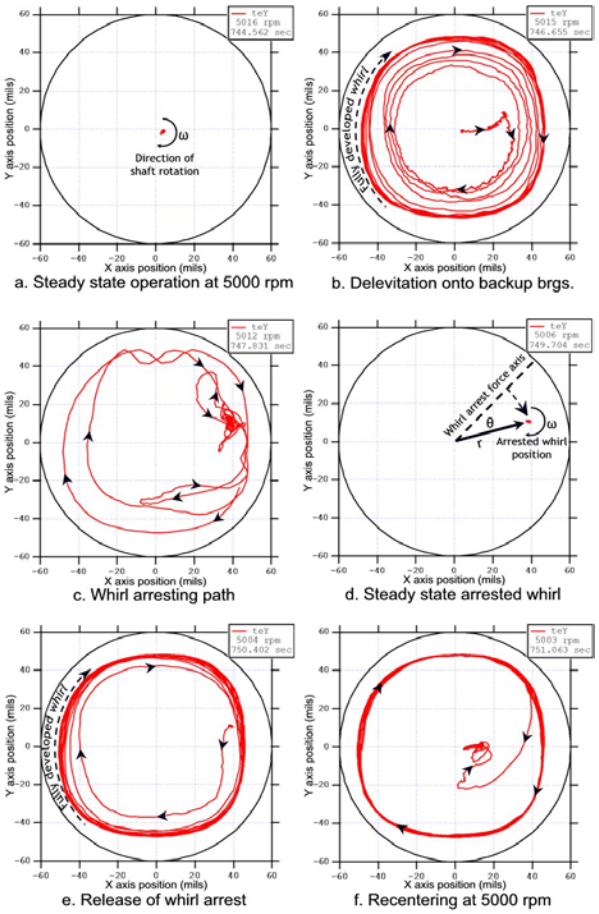

Figure 7a-f. Dropping, arresting, and relevitating rotor at 5000 rpm

Figures 7a-f show the operation of the whirl arrest circuit capturing the rotor during a 5000 rpm drop test. For this experiment, the rotor was delevitated intentionally by the magnetic bearing controller, and whirl was allowed to fully develop before activating the whirl arrest circuit. The circuit has the immediate effect of influencing the orbit shape to non-circular, and after 3-4 whirl cycles (150 ms), holding the rotor steadily against the backup bearings in quadrant 1. The rotor is then dropped again onto the backup bearings, allowing whirl to fully develop, then relevitated to center. Note, one second of time data is shown in each plot.

An extremely significant point regarding the whirl arrest behavior is the angular location at which the rotor

settles after being captured. When using the whirl arrest at rest, the rotor pulls directly toward the 45° position in quadrant 1 (indicated by the dashed line in Figure 5). However, at 5000 rpm, the lock in position *leads* the 45° line by an angle θ, of approximately 30°. This fact indicates that there is a constant, forward directed force which opposes and exceeds that of the backup bearing drag. As summarized in Table 1, this phase angle does not vary significantly with drop speed, suggesting that the rise of the forward acting force is essentially balanced with the rise of the retarding bearing drag.

Table 1. Summary of arrested position of spinning rotor

Shaft Speed	Arrest Current	Thrust End Bearing Arrested Position	
ω at Drop (rpm)	(dc A)	r Radial Position (mils)	θ Lead Angle (°)
500	1.2	41.4	40.3
1000	1.75	41.1	42.4
1500	4	41.8	34.0
2000	5	42.9	31.8
2500	5	42.7	31.9
3000	5	42.4	28.0
4000	5	41.6	28.5
5000	5	39.9	29.6

The demonstration of a forward acting force is important as it is likely the root cause of forward whirl in this rotor. A possible explanation for the origin of this forward acting force is damping in the rotating assembly [17]. The radial bearing lamination stacks provide an obvious potential source of damping in the sliding frictional interfaces between the individual laminations.

Due to the particular geometry of the ALPS flywheel rotor, the radial bearing permanent magnet bias force not only presses the rotor against the backup bearings, but also induces a large bending moment in the bearing lamination area of the shaft, likely exacerbating frictional damping between the laminations. The rotor lamination areas are in fact located in the large deflection regions of the shaft, where any damping effect would be most significant. The main body of the rotor, with its large composite structure, may also be a source of damping specific to the ALPS rotor, although this is not a region of large deflection. It should be noted that the amount of damping required for this theory is not necessarily high, only enough to dominate over the relatively low rotational drag of the ball backup bearings.

High internal damping in the rotor lamination stacks is a theory that may explain the rotor's tendency to forward whirl, rather than to reverse whirl, as exhibited by many smaller, rigid rotors. Perhaps the ALPS rotor's ratio of relatively high internal shaft damping and relatively low backup bearing drag provide the necessary conditions for forward whirl on the backup bearings. Therefore, perhaps a flexible rotor with a relatively high amount of internal shaft damping (which is traditionally avoided in conventionally supported rotors) is actually desirable in preventing high frequency reverse whirl in magnetically supported rotors operating on their backup bearings. Future drop simulations will incorporate a forward driving force due to damping in the rotating assembly to attempt to replicate the behavior observed during the drop experiments.

The theory of lamination frictional damping driving forward whirl can be tested by "bias field cancellation", an alternative whirl arrest method that was conceived, but not yet attempted. As the permanent magnet bias increases deflection in the lamination region of the shaft (and therefore damping force magnitude), reducing the bias field should decrease the tendency to forward whirl. By passively reducing or canceling the radial bearing permanent magnet bias field through commanding opposing dc currents in the control coils, the rotor is expected to transition from forward whirl to reverse whirl while on the backup bearings. By selecting the appropriate level of bias field cancellation current, the forward whirl force may be reduced to the point that it balances against the backup bearing drag, resulting in zero whirl.

FUTURE WORK

Upon completion of the endurance tests in progress, an accurate characterization of the magnetic bearing losses will be performed by integrating the experimental temperature data with the thermal analysis model. In parallel, commissioning and tuning to full speed will be performed over the coming weeks, thus concluding intermediate spin testing.

The next phase of ALPS flywheel testing will take place after the remaining composite rings are installed, building the rotor to its final 5100 lb form. The full rotor, full power testing with the motor generator will be performed first statically in the laboratory, before integration into the locomotive. The dynamic demonstration of the complete ALPS power system in locomotive operation on a test track is currently scheduled for the 4th quarter of 2005.

ACKNOWLEDGEMENTS

This material is based upon work supported by Federal Railroad Administration cooperative agreement, DTFR53-99-H-00006 Modification 4, dated April 30, 2003. Any opinions, findings, and conclusions or recommendations expressed in this publication are those of the authors and do not necessarily reflect the view of the Federal Railroad Administration and/or U.S. DOT.

The authors would also like to acknowledge the numerous colleagues and partners who have made contributions to the development of the ALPS flywheel, without which these experiments would not have been possible. Recognition goes in particular to CEM engineers Doug Wardell, Carl Graf, and Jim Upshaw

for engineering the control and instrumentation equipment of the experiments, overseeing the composite ring fabrication, and carrying out the precise assembly of the flywheel components, respectively. Special appreciation is given to former CEM employee Bobby Sledge for his many years of diligent design and fabrication work on the flywheel. Larry Hawkins of Calnetix deserves thanks for his excellent work in designing an AMB compensator to integrate with existing hardware. Finally, gratitude is offered to Dr. Alan Palazzolo and his VCEL group at Texas A&M University for their work in simulating and optimizing the actuator design for controllability, and support during early flywheel commissioning.

BIBLIOGRAPHY

[1] Herbst, J.D., Caprio, M.T., Thelen, R.F., "Status of the Advanced Locomotive Propulsion System (ALPS) Project," 2003 ASME International Mechanical Engineering Congress & Exposition (IMECE '03), November 16-21, 2003, Washington D.C.

[2] Caprio, M.T., Herbst, J.D., Thelen, R.F., "2 MW 130 kWh Flywheel Energy Storage System," Electrical Energy Storage Applications and Technology (EESAT2003), October 27-29, 2003, San Francisco, CA.

[3] Thelen, R.F., Herbst, J.D., Caprio, M.T., "A 2MW Flywheel for Hybrid Locomotive Power," IEEE Semiannual Vehicular Technology Conference, October 6-9, 2003, Orlando, FL.

[4] Murphy, B.T, Ouroua, H., Caprio, M.T., Herbst, J.D., "Permanent Magnet Bias Homopolar Magnetic Bearings for a 130 kW-hr Composite Flywheel," ISMB-9, August 3-6, 2004, Lexington, KY.

[5] Fumagalli, M.A., *Modelling and Measurement Analysis of the Contact Interaction between a High Speed Rotor and its Stator*, Dissertation ETH No. 12509, Swiss Federal Institute of Technology, Zurich, 1997.

[6] Bartha, A.R., *Dry Friction Backward Whirl of Rotors*, Dissertation ETH No. 13817, Swiss Federal Institute of Technology, Zurich, 2000.

[7] Maslen, E.H., Barrett, L.E., "Feasible Whirl of Rotors in Auxiliary Bearings," UVA MAG 1995.

[8] Schmied, J., Pradetto, J.C., "Behaviour of a one ton Rotor Being Dropped into Auxiliary Bearings," ISMB 1992.

[9] Swanson, E.E., Kirk, R.G., Wang, J., "AMB Rotor Drop Initial Transient on Ball and Solid Bearings," UVA MAG 1995.

[10] Kirk, R.G., Ishii, T., "Transient Rotor Drop Analysis of Rotors following magnetic bearing Power Outage," UVA MAG 1993.

[11] Foiles, W.C., Allaire, P.E., "Nonlinear Transient Modeling of Active Magnetic Bearing Rotors during Rotor Drop on Auxiliary Bearings," UVA MAG 1997.

[12] Fumagalli, M., Schweitzer, G., "Motion of a Rotor in Retainer Bearings," ISMB 1996.

[13] Ishii, T., and Kirk, R.G., "Transient Response technique Applied to Active Magnetic Bearing Machinery During Rotor Drop," ASME Biennial 1991.

[14] Bartha, A.R., "Dry Friction Backward Whirl of Rotors: Theory, Experiments, Results, and Recommendations," ISMB 2000.

[15] Hawkins, L.A., Flynn, M., "Influence of Control Strategy on Measured Actuator Power Consumption in an Energy Storage Flywheel with Magnetic Bearings," 6th International Symposium on Magnetic Suspension Technology, October 7-11, 2001, Torino, Italy.

[16] Kirk, R.G., Ishii, T., "Analysis of Rotor Drop on Auxiliary Bearings Following AMB Failure," UVA MAG 1991.

[17] Black, H.F., "The Stabilizing Capacity of Bearings for Flexible Rotors with Hysteresis," ASME Paper No. 75-DET-55, Design Engineering Technical Conference, Washington D.C., September 1975.

Additional references reviewed but not cited

[18] Ramesh, K., Kirk, R. G., "Rotor Drop Test Stand for AMB Rotating Machinery Part II: Steady State Analysis and Comparison to Experimental Results," ISMB 1994.

[19] Raju, K.V.S., Ramesh, K., Swanson, E.E., Kirk, R.G., "Simulation of AMB Turbomachinery for Transient Loading Conditions," UVA MAG 1995.

[20] Tessier, L.P., "The Development of an Auxiliary Bearing Landing System for a Flexible AMB-Supported Hydrogen Process Compressor Rotor," UVA MAG 1997.

[21] Ecker, H., "Steady-State Orbits of an AMB-Supported Rigid Rotor Contacting the Backup Bearings," UVA MAG 1997.

[22] Feeny, B., Fumagalli, M., Schweitzer, G., "Dynamics of Rigid Rotors in Retainer Bearings," ISMB 1992.

[23] Dell, H., Engel, J., Faber, R., Glass, D., "Developments and Tests on retainer Bearings for Large Active Magnetic Bearings," ISMB 1988.